

Microfabricated Inductors for 20 MHz Dc-Dc Converters

T. O'Donnell¹, N. Wang¹, R. Meere¹, F. Rhen¹, S. Roy¹, D. O'Sullivan², C. O'Mathuna¹

¹Tyndall National Institute,
Lee Maltings, Prospect Row
Cork, Ireland.

²Power Electronics Research Lab, University College Cork,
Cork, Ireland.

Abstract-This paper presents the design and measured results for micro-fabricated inductors suitable for use in high frequency (> 10 MHz), low power (1 –2 W) dc-dc converters. The design has focused on maximizing inductor efficiency for a given converter specification. Inductors in the range of 100 nH to 300 nH have been fabricated and tested. The small signal measurements show a relatively flat inductance profile, with a 10% drop in inductance at 30 MHz. Inductance vs. dc bias current measurements show less than 15% decrease in inductance at 500 mA current. The performance of the micro-inductors have also been compared to a conventional wire-wound inductor in a 20 MHz dc-dc converter. The converter efficiency is shown to be approximately 4% lower when the micro-inductor is used compared to the when the wire-wound inductor is used. The peak efficiency of the micro-inductor in the converter is estimated to be approximately 93%.

I. INTRODUCTION

With the increasing requirement for voltage conversion in portable electronics equipment, miniaturization and integration of the dc-dc converter is becoming an area of intense interest. Although there has been considerable recent progress in the integration of the active parts of such converters, significant miniaturization of the overall converter is retarded by the need to miniaturize and integrate the passive components. The size of the passive component is related to its value and the required value of inductance and capacitance can only be decreased by using higher switching frequency for the converter. Although all of today's low power converter products have switching frequencies less than 10 MHz, recent research has presented converters with frequencies as high as 480 MHz [1], and 100 MHz [2][3]. At such frequencies the values of inductance required are small and integration of the inductor on to the IC or into the package, using micro-fabrication techniques may be practical. By micro-fabrication techniques, here we mean the use of low temperature processes, which are in principle compatible with direct fabrication of the inductor on the active components. Although significant previous work has been done on integrated micro-fabricated inductors [4]-[11] for power conversion applications, much of this work has focused on the frequency range of less than 10 MHz. A detailed review of previous work in micro-inductor components has been given in [12]. Notable examples of this work include the work of Nakazawa et al [5] which demonstrated the direct integration of a micro-inductor on top of an active circuit. Orlando et al. [9] demonstrated a micro-fabricated inductor with the highest reported inductance to dc resistance ratio and Prabhakaran et al. demonstrated low value (several nH) micro-inductors with high current handling capability (up to 10 A). To be a practical alternative to conventional inductor technology, the micro-inductor technology must be implemented in a cost effective manner and size is an important consideration for cost-effectiveness. The cost of the final micro-fabricated devices is related to the number of steps used in the fabrication and the substrate area occupied by a device. For example in [9] the high inductance to dc resistance was achieved in a relatively large area of 5.6 x 5.6 mm² and with a relatively complex process. The fully integrated device reported in [5] was made with a sputter deposited 9 μm thick layer of magnetic material, which may not be cost effective in practice. In general it is unlikely that in portable products, where battery lifetime is an important issue, that increased losses will be acceptable even for a more miniaturized solution. Thus the performance of any integrated solution must be adequate and comparable to existing solutions. It is clear then that further improvement in micro-inductor size and efficiency are desirable, over what has previously been reported.

The size of the micro-inductor is reduced as the frequency is increased due to the need for a smaller inductance. In this work we target an inductor operating frequency of 20 MHz, which is higher than much of what has been previously reported.

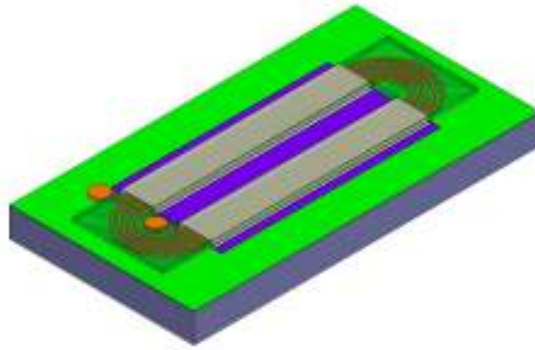


Figure 1: Drawing of a micro-inductor, on a Silicon substrate.

It is critical, however that as frequency is increased, the inductor performance does not decrease. From the performance perspective the challenge is to achieve adequately low losses in the micro-fabricated coils and in the core materials as frequency is increased. We present results for inductors with efficiency greater than 90% when used in a 20 MHz dc-dc converter. The remainder of the paper is laid out as follows. In section II the inductor technology is briefly discussed. Section III presents the approach to the inductor design in order to achieve good performance. Section IV presents measured results for inductor performance up to 100 MHz and also presents results for the use of the inductors in a 20 MHz dc-dc converter. The losses in the inductors is analyzed and compared to conventional technology. Section V draws some conclusions from the work and indicates the direction for future work.

II. INDUCTOR TECHNOLOGY

A detailed description of the technology used to fabricate the inductors has been given previously [13]. The essential details which are required in order to understand the design process are briefly described here. The inductor consists of a racetrack shaped copper coil, which is surrounded by a layer of magnetic material. The coil consists of electroplated copper which can be deposited to a maximum thickness of 50 μm . The magnetic material is an alloy of Nickel and Iron, which is also deposited by electroplating. The thickness of the layer of magnetic material is determined by the design, and is generally limited to less than 10 μm due to considerations of limiting the eddy current loss. The entire process consists of 5 mask layers.

This racetrack inductor construction has been chosen over other inductor constructions (such as a toroidal approach) because of its relatively simple construction, which requires just a single layer of conductors, thus avoiding the use of vias.

The direction of flux travel in the device is in a single direction, perpendicular to the long axis of the core, which allows for the exploitation of anisotropy in the material, to reduce core losses. The core material is deposited in the presence of a magnetic field which induces an anisotropy, i.e. a hard and easy axis of magnetization in the material. The easy axis is induced parallel with the core long axis, so that during inductor operation the flux travel is along the hard axis. In the hard axis, magnetization takes place by domain rotation as opposed to domain growth. Domain rotation is a low loss mechanism, so that exploiting material anisotropy is an important technique for reduction of core loss for high frequency operation.

III. INDUCTOR DESIGN

There are several figures of merit which could be considered to indicate good inductor performance. For micro-fabricated inductors the quality factor, Q , is frequently used. However the Q-factor, which the ratio of inductor reactance ($2\pi fL$) to resistance (R) at a particular frequency, f , only gives information on the AC performance of the inductor. For inductors used in power conversion, the inductor excitation current waveform will typically have a considerable dc component. Thus the inductor dc resistance, R_{dc} , is also an important factor and some works [9] have identified the ratio of inductance, L , to dc resistance as a measure for good power inductor performance.

In order to optimize the performance of a power inductor, it is clear that losses due to both the dc and ac components of current must be minimized. Thus in this work we choose the inductor efficiency as a figure of merit and the objective of the inductor design is to maximize inductor efficiency with the given technology parameters. Inductor efficiency is defined as

$$\eta_{ind} = P_{out}/(P_{out} + P_{loss}) \quad (1)$$

where P_{out} is the converter output power and P_{loss} is the total inductor loss. The inductor loss includes winding loss and core loss. Since the inductor waveform consists of a triangular wave with a dc level, the winding loss consists of both ac and dc components. The core loss is due to the triangular ac component of the excitation and consists of both hysteresis loss and eddy current loss. A modeling procedure has been developed for the inductor, which given the geometry and the material parameters, and the excitation, evaluates all the loss components in the inductor and hence estimates the inductor efficiency. The winding ac loss is estimated using an analytic method which takes into account the 2-d nature of fields in the winding window. Losses due to current waveform harmonics up to the 6th harmonic are included by use of the Fourier series expansion of the current waveform. The eddy current core loss is evaluated using a 1-d solution for Maxwell's equations within the core cross-section [14]. The hysteresis loss is determined from measurements on toroidal samples of the core material and is approximated by the Steinmetz equation.

The inductors are designed to operate in a buck converter with specifications shown in the Table 1. Certain parameters relating to the technology are fixed by the materials and processes used. These fixed parameters are also given in Table 1 below. In order to maximize the inductor efficiency, the number of turns, N , conductor width, w , and core layer thickness, t , and footprint area, A_r , are varied.

TABLE 1: CONVERTER SPECIFICATIONS AND FIXED PARAMETERS RELATING TO THE TECHNOLOGY.

Converter specifications		Fixed parameters	
Input voltage, V_{in}	3 – 5V	Maximum conductor thickness	60 μm
Output voltage, V_{out}	1.2 V	Conductor spacing	50 μm
Output current, I_{out}	500 mA	NiFe effective permeability	280
Ripple current ratio, I_r	< 0.4	NiFe resistivity	45 $\mu\Omega\text{ cm}$
Switching frequency	20 Mhz	NiFe saturation	1.5 T

The inductance value is allowed to vary, but with the constraint that the current ripple does not exceed the specified value. Optimum inductor designs are determined by finding the combination of the above values which gives maximum efficiency for any given footprint area. The graphs in fig. 2 gives an example of how inductor efficiency varies with number of turns, and conductor width for a footprint area varying from 4 mm^2 to 16 mm^2 , and a current ripple ratio of less than 0.6.

It can be seen from the graph that there is a trade-off between footprint area and inductor efficiency. At smaller sizes efficiency tends to decrease. In order to obtain the inductance in a smaller size, the conductor width and spacing is decreased. This results in the decrease in efficiency because of increased winding loss as the cross-sectional area of the conductors is decreased. At some point the inductor size and hence the core area and effective length is reduced to the point where the required peak current cannot be handled without core saturation. This presents an ultimate limit to the smallest size for the inductor, and in the above graphs, this occurs at a footprint area of approximately 4 mm^2 . It should however be noted that at this minimum size, inductor efficiency has decreased to approximately 86 %. The above approach has been used to design several inductors with different inductance values. Design parameters were varied and the maximum efficiency designs for each footprint area were identified. Inductor designs were picked in order to maintain efficiency above 90% rather than to minimize footprint area. The next section describes some of the inductor designs and the measured results from these.

IV. RESULTS

A range of inductors have been fabricated and an image of several different variants of the inductors is shown in fig. 3 below. The design details for a 100 nH, 200 nH and 300 nH inductor are given in table 2.

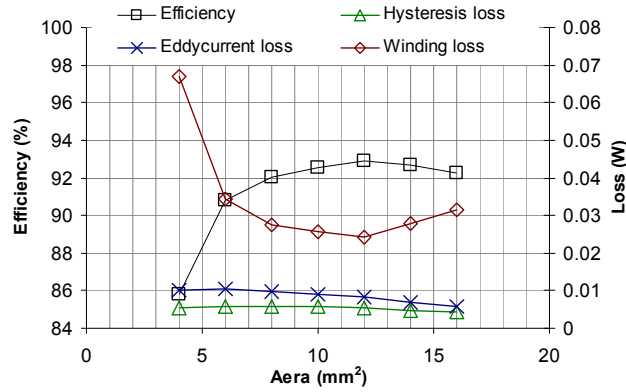


Figure 2: Measured inductance and resistance of three fabricated micro-inductors.

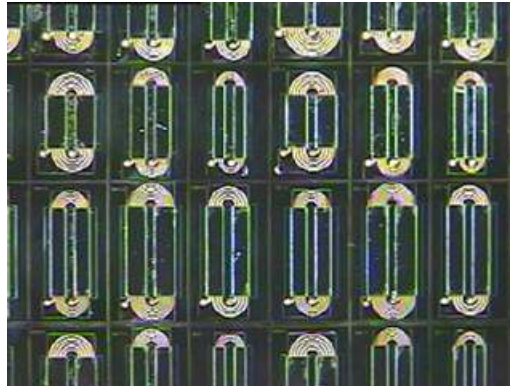


Figure 3: Microfabricated inductors

TABLE 2: DESIGN DETAILS FOR THE FABRICATED MICRO-INDUCTORS.

L (nH)	N	Area (mm ²)	R _{dc} (Ω)
100	4	6.4	0.133
200	7	9.35	0.218
300	5	8.51	0.43

A. Small Signal Testing

The inductance and resistance have been measured vs. frequency, up to 100 MHz, using a vector network analyzer. The graph in fig. 4 below shows the results for the three inductors with inductance values of 100 nH, 200 nH and 300 nH. It can be seen from the graph that the inductance is relatively flat up to 20 MHz with an inductance decrease of approximately 10 % at 30 MHz. The self resonant frequencies (SRF) of the inductors are all greater than 100 MHz. The SRF of the 100 nH, 200 nH and 300 nH inductors are 740 MHz, 380 MHz and 230 MHz respectively. The measured dc resistances are 0.133 Ω, 0.218 Ω, and 0.43 Ω for the 100 nH, 200 nH and 300 nH inductors respectively. It can be seen that the resistance of the inductors increases significantly for frequencies above 20 MHz and this increase is largely due to eddy current loss in the core.

When used in a power converter the inductor must also be capable of carrying the maximum converter dc current while maintaining the inductance level, i.e. without core saturation. Fig. 5 presents the inductance (at 20 MHz) vs. dc bias current for the inductors. It can be seen that inductance hold up well with bias current and the inductance roll off is relatively gentle. At 500 mA the reduction in inductance value is less than 15 % in all cases.

B. Tests in a Converter

Testing of the inductors in a 20 MHz converter has also been carried out. Fig. 6 shows an image of the converter chip and the micro-fabricated inductor. The inductor used is a 100 nH inductor.

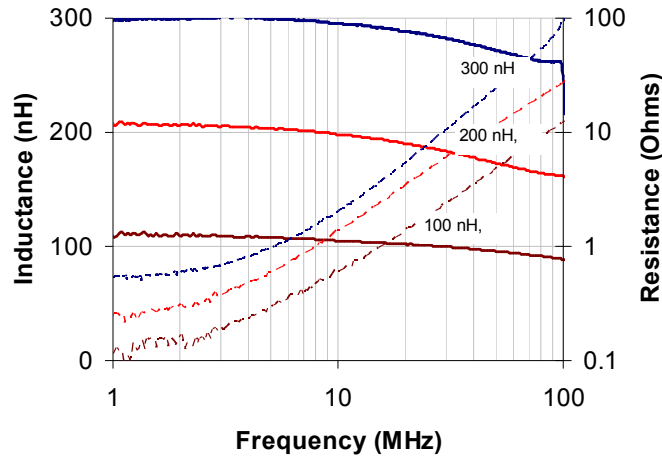


Figure 4: Measured inductance and resistance of three fabricated micro-inductors.

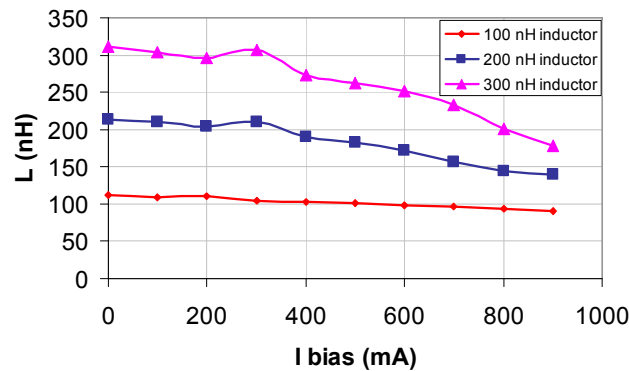


Figure 5 : Measured inductance at 20 MHz vs. dc bias current of the three fabricated micro-inductors.

Details of the converter design can be found in [15]. In order to benchmark the micro-inductor performance the efficiency of the converter using the micro-inductor has been compared to the efficiency of the converter using a conventional wire-wound inductor (Coilcraft 0805 LS-111, $L = 110$ nH, $R_{dc} = 50$ m Ω). Fig. 7 shows the measured efficiency of the converter vs. load current with both inductors. Converter input voltage is 2.6 V and output voltage is 1.2 V. It can be seen from this that the peak efficiency of the converter with the wirewound inductor is approximately 4 % higher than with the micro-inductor. Using the models developed for the micro-inductor and using the inductors models supplied by Coilcraft, the inductor efficiency in this converter can be estimated. These curves for inductor efficiency are also included in fig. 7. The inductor efficiency curves are consistent with the measured converter efficiency, in that the efficiency of the micro-inductor is shown to be approximately 3% lower than that of the wire-wound inductor. The peak micro-inductor efficiency is approximately 93%. In order to further illustrate the reason for the difference in efficiency between the inductors, the graph in fig. 8 shows the breakdown of losses in the inductors as obtained from the models.

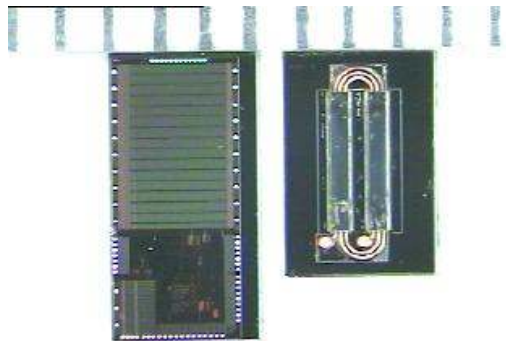


Figure 6 : Image of 100 nH micro-fabricated inductor and 20 MHz DC-DC converter IC. The scale at the top is in mm.

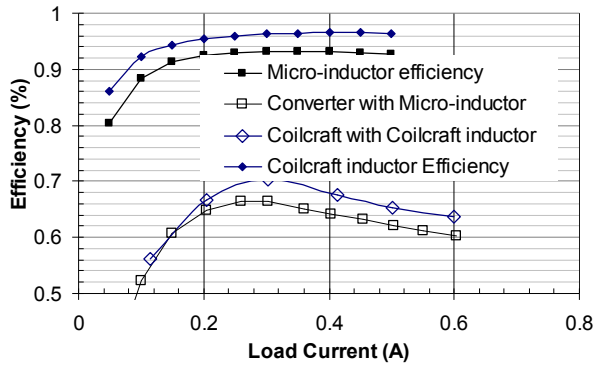


Figure 7 : Measured efficiency for the 20 MHz converter comparing efficiency with the micro-inductor and efficiency with the wire-wound inductor.

The loss has been separated into ac loss and dc loss. Due to the nature of the wire-wound inductor model it is not possible to further separate the ac loss into core loss and winding loss. The loss breakdown shows that the wire-wound inductor has lower ac loss and lower dc loss. AC loss dominates in both inductors at low current levels as expected. For the micro-inductor dc loss exceeds ac loss at higher current levels. For the micro-inductor the loss can also be examined in terms of the split between winding loss (both ac and dc) and core loss.

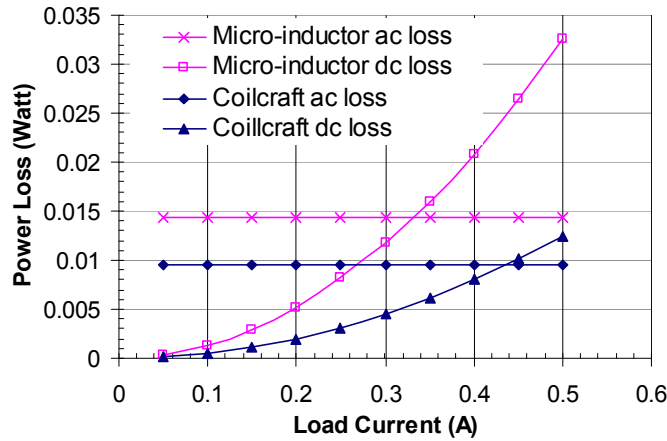


Figure 8 : Plot of AC and DC loss for the micro-inductor and the wire-wound inductor.

The diagram in fig. 9 shows the breakdown of losses in the micro-inductor for a current of 250 mA. This shows that the winding loss is substantially dc loss and that the core loss is dominated by eddy current loss.

V. CONCLUSIONS

This paper has presented the design and measurement of micro-inductors for use in a 20 MHz dc-dc converter. Inductor performance has been analyzed in terms of inductor efficiency. The micro-inductors have been shown to have a peak efficiency of approximately 93% and are 3-4% less efficient than a conventional wire-wound inductor.

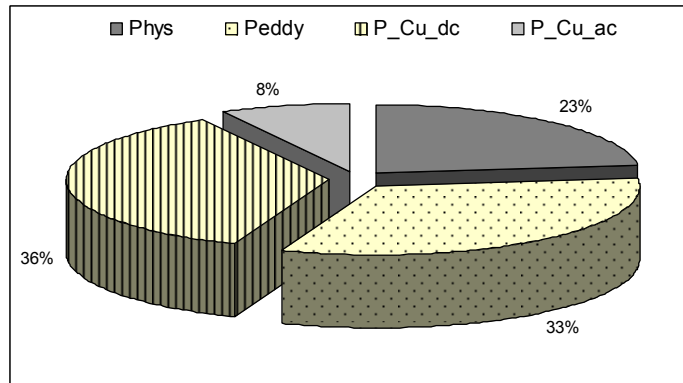


Figure 9: Breakdown of losses in the micro-inductor for 250 mA dc current.

Although the micro-inductor efficiency is still less than that of the wire-wound inductor, the results show that the performance difference is not very large. From an analysis of the losses in the micro-inductor it is clear that both winding and core loss needs to be further reduced. The winding loss is mostly due to winding dc resistance and this could be further reduced by increasing the conductor thickness. The conductor thickness is currently 50 μm , but it may be possible to increase this to 100 μm . Process improvements required to do this are currently being investigated. The core loss is dominated by eddy current loss. This can be reduced by a combination of higher resistivity core material, such as alloys of Cobalt and Phosphorous, and by laminating the core [16]. Both of these options are currently being pursued.

The main reason for considering the use of a micro-inductor solution in a converter is to achieve a size reduction. It is unlikely that the micro-inductor technology can compete with conventional inductor technology (e.g. wire-wound or multi-layer ferrite) in terms of inductance per unit area. However the profile of the micro-inductor is significantly lower than that of conventional inductors. The micro-inductor has a profile of less than 0.2 mm, while most chip inductors have profiles greater than 0.5 mm. The greatest size reduction in a converter can be achieved by the stacking of the passive and active components and in such a scenario the low profile of the micro-inductor has a distinct advantage.

ACKNOWLEDGMENT

The authors wish to acknowledge the support of Enterprise Ireland in funding this work under the Industry Led Research Programme, ILRP/PEIG/05.

REFERENCES

- [1] Gerhard Schrom, Peter Hazuchii, Jaehong Hahn, Donald S. Gardner, Bradley A. Bloechel, Greg Dermer, Siva G. Narendra, Tanay Kamik., "A 480-MHz, Multi-Phase Interleaved Buck DC-DC Converter with Hysteretic Control", 2004 35th Annual IEEE Power Electronics Specialists Conference Aachen, Germany, 2004, pp. 4702-4707.
- [2] G. Schrom, P. Hazucha, F. Paillet, D. J. Rennie', S. T. Moon, D. S. Gardner, T. Kamik, P. Sun, T. T. Nguyen, M. J. Hill, K. Radhakrishnan, T. Memioglu, "A 100MHz Eight-Phase Buck Converter Delivering 12A in 25mm² Using Air-Core Inductors", IEEE 22nd Annual Applied Power Electronics Conference, APEC 2007, February 2007, pp. 727-730.
- [3] Vincent Pinon, Bruno Allard, Christophe Garnier, "High-Frequency Monolithic DC/DC Converter for System-on-Chip Power Management", Proceedings of the 18th International Symposium on Power Semiconductor Devices & IC's, June 4-8, 2006 Naples, Italy.
- [4] Jae Yeong Park, Suk H. Han, and Mark G. Allen, "Batch-Fabricated Microinductors with Electroplated Magnetically Anisotropic and Laminated Alloy Cores", IEEE Transactions On Magnetics, Vol. 35, No. 5, September 1999.
- [5] H. Nakazawa, M. Edo, Y. Katayama, M. Gekinozu, S. Sugahara, Z. Hayashi, K. kuroki, E. Yonezawa, and K. Matsuzaki, "Micro-DC/DC Converter that Integrates Planar Inductor on Power IC", IEEE Transaction on Magnetics, Vol. 36, No. 5, September 2000, pp. 3518-3520.
- [6] Y. Fukuda, T. Inoue, T. Mizoguchi, S. Yatabe and Y. Tachi, "Planar Inductor With Ferrite Layers for DC-DC Converter", IEEE Transactions on Magnetics, Vol. 39, No. 4, July 2003, pp. 2057-2061.
- [7] T. Sato, K. Yamasawa, H. tomita, T. Inoue, T. Mizoguchi, "Planar Power Inductor using FeCoBN Magnetic Film with High Saturation Magnetization and High Electrical Resistivity", Proceedings of the International Power Electronics Conference, IPEC'00, Tokyo, 2000, pp. 303-308.
- [8] M. Yamaguchi, H. Okuyama, and K. I. Arai, "Characterisations of Magnetic Thin-Film Inductors at Large Magnetic Filed", IEEE Transactions On Magnetics, Vol. 31, No. 6, November 1995, pp. 4229-4231.
- [9] B. Orlando, R. Hida, R. Cuchet, M. Audoin, B. Viala, D. Pellissier-Tanon, X. Gagnard, and P. Ancey, "Low-Resistance Integrated Toroidal Inductor for Power Management", IEEE Transactions On Magnetics, Vol. 42, No. 10, October 2006, pp. 3374-3376.
- [10] Satish Prabhakaran, Yuqin Sun, Parul Dhagat, Wei-dong Li and Charles R. Sullivan, "Microfabricated V-Groove Power Inductors for High-Current Low-Voltage Fast-Transient DC-DC Converters", IEEE 36th Power Electronics Specialists Conference, 2005. PESC '05. pp.1513 – 1519.
- [11] XiaoYu Gao, Yong Zhou, Wen Ding, Ying Cao, Chong Lei, Ji An Chen, and Xiao Lin Zhao, "Fabrication of Ultralow-Profile Micromachined Inductor With Magnetic Core Material", IEEE Transactions On Magnetics, Vol. 41, No. 12, December 2005, pp. 4397-4400.
- [12] S.C. O'Mathuna, T. O'Donnell, N. Wang, K. Rinne, 'Magnetics on Silicon an Enabling Technology for Power Supply on Chip', IEEE Transactions on Power Electronics, vol. 20, no. 3, May 2005, pp585-592.
- [13] Ningning Wang, Terence O'Donnell, Saibal Roy, Paul McCloskey, Cian O'Mathuna, "Micro-inductors Integrated on Silicon for Power Supply on Chip", Journal of Magnetism and Magnetic Materials, 316 (2007), e233–e237.
- [14] Ferromagnetism, Richard M. Bozorth, IEEE Press, 1993.
- [15] J. Hannon, D. O'Sullivan, J.Griffiths,R. Foley, K. McCarthy and M. Egan, "Design of a High Efficiency 2 A High Frequency Buck Converter", Proc. IEEE Applied Power Electronics Conference, APEC 2008, Austin, TX, Feb. 24-28, 2008.
- [16] M. Brunet, T. O'Donnell, A.M. Connell, P. McCloskey, S.C. O'Mathuna, "Electrochemical Process for the Lamination of Magnetic Cores in Thin-Film Magnetic Components", Journal of Microelectromechanical Systems, vol. 15, no. 1, Feb 2006, pp 94-10.